2018 IEEE Workshop on Modeling and Control in Power Electronics (COMPEL 18)

Resonant Converter Design Using Two-Port Passive Network: Single Frequency Design

Euihoon Chung, Gyu Cheol Lim, and Jung-Ik Ha
Dept. of Electrical and Computer Engineering
Seoul National University
Seoul, Korea
E-mail: ystar55@snu.ac.kr and jungikha@snu.ac.kr

David J. Perreault
Massachusetts Institute of Technology
Cambridge, MA 02139, USA

***Abstract*— This paper proposes a design method of resonant converter through two-port network analysis. The impedance conversion characteristics of a two-port network consisting solely of passive elements are analyzed at a single frequency. Through this analysis, this paper presents a general method of designing resonant networks that satisfy the desired input- and output-specifications under the rated conditions and has the desired characteristics for load variations. This design method allows designers to configure resonant networks suitable for specific applications without relying on case studies. To verify the proposed design concept, design examples are introduced and simulation results are provided.**

Keywords—resonant converter, resonant network, two-port passive network

I. INTRODUCTION

Resonant converters have been widely used for high-frequency power conversion due to the soft switching operation such as zero voltage switching (ZVS) and zero current switching (ZCS). Fig. 1 shows a common structure of a resonant converter which consists of an inverter, a resonant network, and a rectifier for a dc-dc power conversion. The inverter stage synthesizes high-frequency ac-voltage from the input dc-voltage source. Conversely, the rectifier stage converts ac-voltage to dc-voltage and delivers dc-power to the load. Between the inverter and the rectifier stages, the resonant network provides transformation of voltage or current level. Therefore, the characteristics of the resonant converter are closely related to the design of the resonant network.

A series resonant converter (SRC) and parallel resonant converter (PRC) are two most simple types of resonant converters which have two passive elements in the resonant network. However, their use is limited as several disadvantages have been pointed out [1, 2]. Accordingly, various topologies consisting of three elements or more elements have been constructed as an alternative. Many existing researches have focused on listing all the possible topologies based on the number of elements and comparing the characteristics of them in order to select a topology suited for a particular application [1-6]. For instance, [6] investigates a family of resonant topologies with three or four passive elements and derives several topologies that exhibit immittance conversion characteristics. However, these approaches have limitation since the number of possible topologies drastically increases as the number of resonant elements increases.

In [7], authors have presented a new viewpoint of designing a resonant network by examining the equivalence relations of several resonant tanks, and introduced the process to simplify the design of higher-order resonant networks.

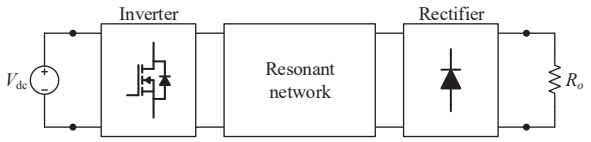

Fig. 1. The common structure of resonant converters.

This paper introduces the guideline to design a resonant network using a two-port network analysis. The aim of this paper is to provide insight into the design of resonant converters by examining the feasibility and limitations of the two-port network analysis. A resonant network is a kind of two-port network that is used as an impedance transform stage. In this paper, the input impedance of a resonant network is derived as a function of the load impedance. This generalized representation of input impedance allows designers to implement resonant networks satisfying the desired characteristics at the input and output ports, without relying on case studies. Although this method can be extended to multi-frequency analysis, this paper focuses on a single-frequency case to explain the proposed design concept, and it is applied to design of a resonant converter operating at a fixed frequency. In order to verify the design concept, two design examples are introduced and simulation results are presented.

II. NETWORK DESIGN WITH TWO-PORT NETWOK THEORY

A. Impedance transformation using two-port network

Under the assumption that a two-port network is lossless, the relationship between the input and output ports is given by

$$\begin{bmatrix} V_1 \\ V_2 \end{bmatrix} = \begin{bmatrix} jX_{11} & jX_{12} \\ jX_{21} & jX_{22} \end{bmatrix} \begin{bmatrix} I_1 \\ -I_2 \end{bmatrix} \tag{1}$$

where V_1 is the input voltage, I_1 is the input current, V_2 is the output voltage, and I_2 is the output current of a two-port network. For reciprocal networks, X_{12} and X_{21} have the same. In this paper, the reciprocal and lossless networks are considered thus X_{21} is substituted by X_{12} in the remaining part of this paper.

The input impedance Z_{in} and the output impedance Z_{out} are defined as

978-1-5386-5541-2/18/$31.00 ©2018 IEEE

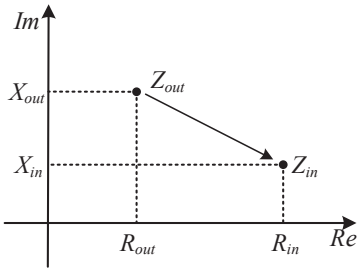

Fig. 2. Impedance transformation in the complex plane.

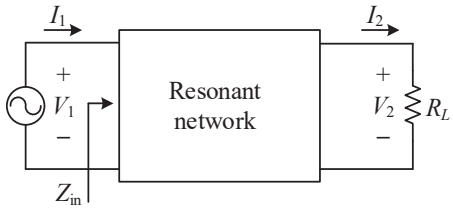

Fig. 3. The simplified model of resonant converters.

$$Z_{in} = V_1 / I_1 = R_{in} + jX_{in},$$
$$Z_{out} = V_2 / I_2 = R_{out} + jX_{out}, \quad (2)$$

where R_{in} is the input resistance, X_{in} is the input reactance, R_{out} is the output resistance, and X_{out} is the output reactance. From (1) and (2), R_{in} and X_{in} are expressed as a function of R_{out} and X_{out} respectively as

$$R_{in} = \frac{X_{12}^2 R_{out}}{R_{out}^2 + \left(X_{out} + X_{22}\right)^2},$$
$$X_{in} = X_{11} - \frac{X_{12}^2 \left(X_{out} + X_{22}\right)}{R_{out}^2 + \left(X_{out} + X_{22}\right)^2}. \quad (3)$$

Using (3), the two-port passive network provides the impedance transformation from Z_{out} to Z_{in} as shown in Fig. 2.

B. Design of resonant converter at the rated condition

Under the fundamental harmonic approximation (FHA), an inverter stage of a resonant converter is considered as an ideal sinusoidal voltage source and a rectification stage is considered as an equivalent load resistance R_L. The value of R_L depends on the rectifier type. For instance, the value of R_L is calculated by $8/\pi^2 R_o$ where the full-wave rectifier is used. Consequently, the structure of the resonant converter in Fig. 1 is simplified as in Fig. 3. Accordingly, the design problem of the resonant converter is simplified by the problem of designing a two-port network with a resistive load R_L. From (3), the load resistance R_L is reflected at the input side as follows,

$$Z_{in} = R_{in} + jX_{in} = \frac{X_{12}^2 R_L}{R_L^2 + X_{22}^2} + j\left(X_{11} - \frac{X_{12}^2 X_{22}}{R_L^2 + X_{22}^2}\right). \quad (4)$$

At the initial stage of converter design, the value of R_L is considered as its rated value R_L^* which is determined at the rated load condition. In order to meet the desired voltage or current conversion, the resonant network needs to be designed so that the target load resistance (R_L^*) is transformed into the desired input impedance ($Z_{in}^*=R_{in}^*+jX_{in}^*$). In other words, the design elements (X_{11}, X_{12}, and X_{22}) of resonant network needs to be selected to satisfy the following equations,

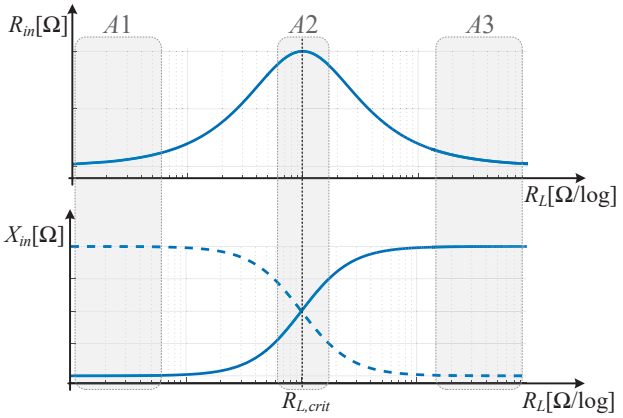

Fig. 4. Input resistance (R_{in}) and input reactance (X_{in}) according to load (R_L) variation.

$$R_{in}^* = \frac{X_{12}^2 R_L^*}{R_L^{*2} + X_{22}^2},$$
$$X_{in}^* = X_{11} - \frac{X_{12}^2 X_{22}}{R_L^{*2} + X_{22}^2}. \quad (5)$$

As shown in (5), only two equations are required while there are three design elements (X_{11}, X_{12}, and X_{22}) when designing a two-port network. Therefore, one remaining degree of freedom can be used for various optimization procedure.

C. Consideration of load variation

Previous subsection *B* deals with converter design in the rated condition. However, the operation of the converter with varying load is also a major concern in converter design. Thus, in this chapter, the remaining degree of freedom is used to satisfy the desired property against load variation.

The graph of R_{in} and X_{in} according to R_L calculated from (4) is generally shown in Fig. 4. This graph intuitively shows the effect of load variation on the input impedance. As shown in the figure, there is the critical point where the first derivative of R_{in} with respect to R_L is zero. The value of R_L at the critical point is defined as $R_{L,crit}$, and it is calculated as

$$R_{L,crit} = \begin{cases} X_{22} & \left(X_{22} \geq 0\right) \\ -X_{22} & \left(X_{22} < 0\right) \end{cases}. \quad (6)$$

When the value of X_{22} has a positive sign, the graph of reactance in figures is represented as a solid line. On the other hand, if the value of X_{22} has a negative sign, the graph of reactance in figures is represented as a dotted line.

This paper introduces the three areas (*A*1, *A*2, and *A*3) which present noticeable characteristics. *A*1 is the area where the target load range is much lower than $R_{L,crit}$ ($R_L << R_{L,crit}$). Under this condition, (4) is simplified as

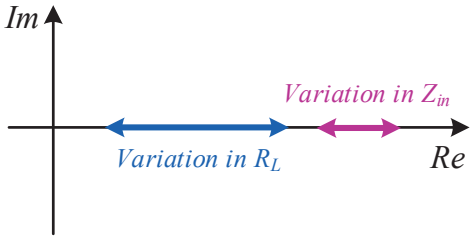

(a)

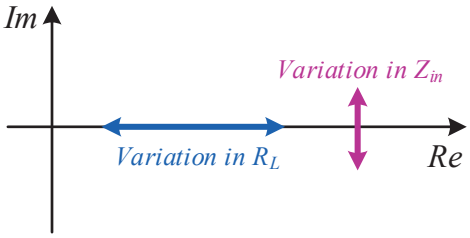

(b)

Fig. 5. Effects of load variation on the input impedance in the complex domain: (a) reactance compression, (b) resistance compression.

$$R_{in} \approx \frac{X_{12}^2}{X_{22}^2} R_L, \quad X_{in} \approx X_{11} - \frac{X_{12}^2}{X_{22}}. \tag{7}$$

Conversely, $A3$ is the area where the target load range is much higher than $R_{L,crit}$ (R_L>>$R_{L,crit}$). Under the condition, (4) is simplified as

$$R_{in} \approx \frac{X_{12}^2}{R_L}, \quad X_{in} \approx X_{11}. \tag{8}$$

In both cases, regardless of load variation, the reactance X_{in} remains in a narrow range. Their characteristics are called as reactance compression and visualized in Fig.5(a) in the complex plane. The difference between $A1$ and $A3$ is the effect of the load variation on R_{in}. As shown in (7), R_{in} is linearly proportional to R_L in $A1$. On the other hand, as shown in (8), R_{in} is inversely proportional to R_L in $A3$. In $A2$, the two-port network reduces the variation of R_{in} when R_L changes as shown in Fig.5(b). Such networks are called resistance compression network (RCN) and are widely used in RF and plasma applications [8, 9]. In [8], the operating principles and implementation of RCN are described in detail.

As aforementioned, the relative position of $R_{L,crit}$ and R_L^* is the crucial design factor to determine the appearance of Z_{in} against load variation. Thus, in this paper, the relative position of them is defined as

$$m = \frac{R_L^*}{R_{L,crit}} = \begin{cases} \dfrac{R_L^*}{X_{22}} & (X_{22} \geq 0) \\ \dfrac{R_L^*}{-X_{22}} & (X_{22} < 0) \end{cases}. \tag{9}$$

Fig. 6 shows the examples where R_L^* is 100 Ω and the desired input impedance Z_{in}^* is 10+j10 Ω (i.e. R_{in}^* is 10Ω and X_{in}^* is 10Ω). Fig. 6(a), (b), and (c) show different cases where the values of m are 0.1, 1.0, and 10, respectively.

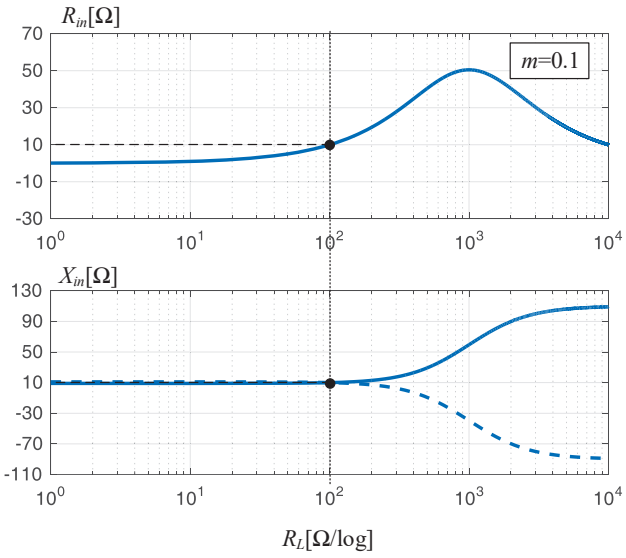

(a)

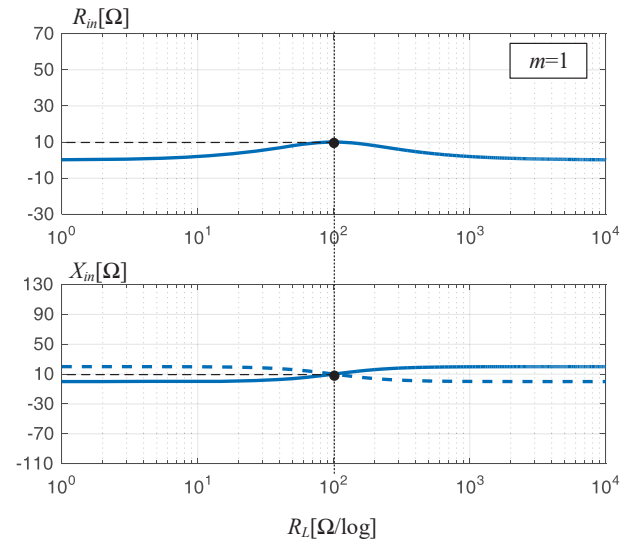

(b)

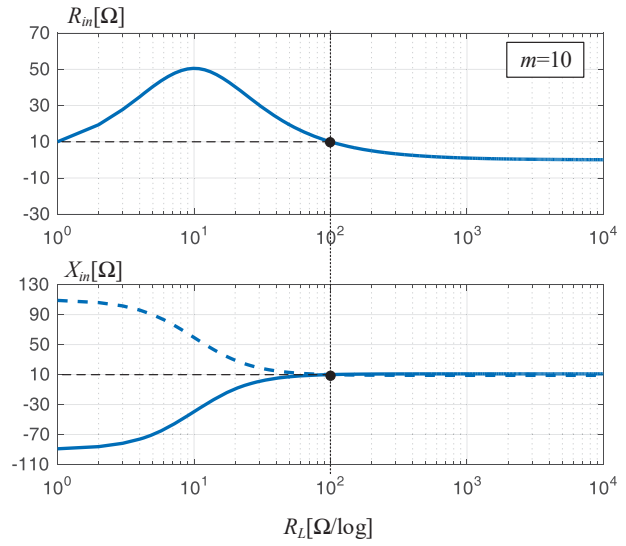

(c)

Fig. 6. The example of input impedance according to load (R_L) where (a)m=0.1, (b)m=1.0, and (c)m=10 while R_L^*(100 Ω) is transformed into Z_{in}^*(10+j10 Ω).

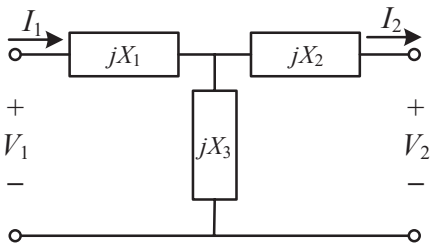

Fig. 7. T-equivalent model of the two-port network.

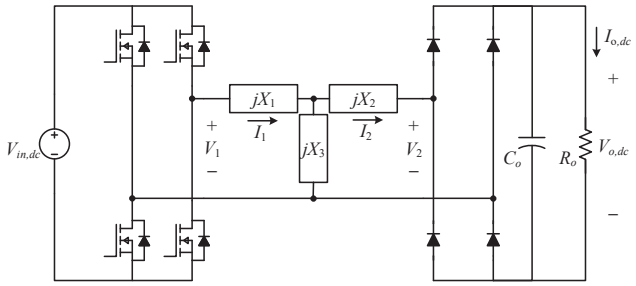

Fig. 8. The configuration of the prototype converter.

Even though the same impedance conversion is performed at one point, it can be seen that the variation in input impedance to the load variation is significantly different depending on the value of m. Even with the same value of m, there are two different options to determine characteristics of input reactance against load variation. For example, when the value of X_{22} is determined as a positive sign (represented as the solid line), the input reactance gradually decreases from the rated value as the load resistance increases from the rated value. Conversely, when the value of X_{22} is determined as a negative sign (represented as the dotted line), the input reactance increases as the load resistance increases. Thus, a designer should take into account the requirements of the application when determining these design factors. When the value of m is selected, the values of three elements (X_{11}, X_{22}, and X_{12}) are determined by one of following two options,

$$\begin{cases} X_{11} = X_{in}^* + \dfrac{R_{in}^*}{m}, \\ X_{22} = \dfrac{R_L^*}{m}, \\ X_{12} = \mp\dfrac{1}{m}\sqrt{\left(1+m^2\right)R_L^* R_{in}^*}. \end{cases} \tag{10-a}$$

$$\begin{cases} X_{11} = X_{in}^* - \dfrac{R_{in}^*}{m}, \\ X_{22} = -\dfrac{R_L^*}{m}, \\ X_{12} = \mp\dfrac{1}{m}\sqrt{\left(1+m^2\right)R_L^* R_{in}^*}. \end{cases} \tag{10-b}$$

When the design factors are determined by (10-a), the value of X_{22} is determined to be a positive value. On the other hand, the value of X_{22} is determined to be a negative value when the design factors are determined by (10-b). In (10-a) and (10-b), the sign of X_{12} does not affect the characteristics at the single frequency. The effect of the sign of X_{12} is discussed in section III.

There are various ways to implement a designed two-port network as an actual circuit. This paper considers the case of implementing the two-port network using the T-equivalent model with three branches as shown in Fig. 7. In the T-equivalent model, the impedance value of each branch is given by

$$\begin{cases} X_1 = X_{11} - X_{12}, \\ X_2 = X_{22} - X_{12}, \\ X_3 = X_{12}. \end{cases} \tag{11}$$

Each branch is replaced by a single reactive element (inductor or capacitor) for a single-frequency design. On the other hand, if the two-port network is designed for multi-frequency, each branch is constructed with multiple reactive elements. For example, when the converter is designed for two frequencies, the branch is configured by either a series or parallel connection of the inductor and the capacitor. When designing at more than two frequencies, branches are realized in various combinations by more passive elements. The multi-frequency analysis is useful when designing a converter with variable-frequency control, or when considering several harmonic components in converter design. However, this paper focuses on the single-frequency optimization to explain the proposed design concept.

III. Results

A. Design examples

In this chapter, two design examples, denoted as P1 and P2, are introduced to verify the proposed design concept. One (P1) is designed to maintain the power factor at the input-port to near unity while the output voltage is kept to the desired value. The other (P2) is also designed to maintain the power factor at the input-port to near unity. On the other hand, in P2, the output current is kept to the desired value. Here, both of them are constructed with the full-bridge inverter and full-wave rectifier, and operated at the fixed frequency which is denoted as f_{sw}. The circuit configuration is shown in Fig. 8. The input- and output-specifications which are desired under the rated condition are listed in Table I. Based on the specifications, the values of R_L^*, R_{in}^*, and X_{in}^* are calculated as

$$\begin{aligned} R_L^* &= \frac{8}{\pi^2}\frac{V_{o,dc}^2}{P_o} = \frac{8}{\pi^2}\frac{P_o}{I_{o,dc}^2}, \\ R_{in}^* &= \frac{8}{\pi^2}\frac{pf^2 V_{in,dc}^2}{P_o}, \\ X_{in}^* &= \frac{8}{\pi^2}\frac{pf\sqrt{1-pf^2}\,V_{in,dc}^2}{P_o}, \end{aligned} \tag{12}$$

The value of X_{in}^* is zero since the unity power factor at the input-port is desired in this example. If it is desired to set the impedance at the input port to be inductive to ensure

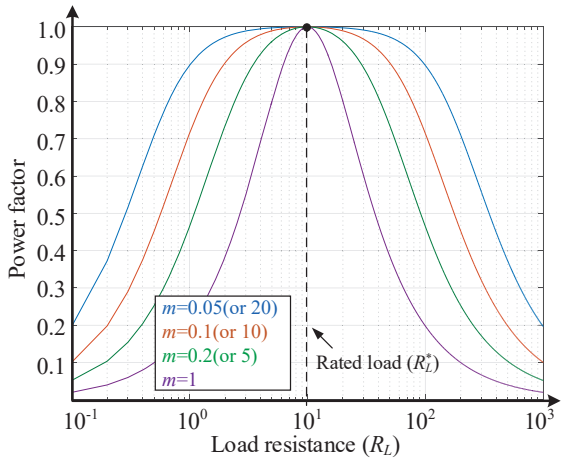

Fig. 9. Power factor according to the values of R_L and m.

TABLE I
THE SPECIFICATION UNDER THE RATED CONDITION

Parameter	Value [Unit]
$V_{in,dc}$	30 [V]
$V_{o,dc}$	24 [V]
$I_{o,dc}$	2 [A]
P_o	48 [W]
pf (input power factor)	~1.0
f_{sw}	100 [kHz]

more reliable operation in ZVS mode, the value of X_{in}^* can be adjusted to a positive value.

As mentioned before, the variation of input reactance can be compressed if the value of m is much lower than 1 ($A1$) or the value of m is much higher than 1 ($A3$). Therefore, if the converter is designed in these areas ($A1$ or $A3$), the input power factor is expected to be close to 1 even with some load variation. When the input power factor deviates slightly from 1 due to load variations, it is desirable that the input impedance be inductive in order to achieve ZVS operation. As shown in Fig. 4, this feature is obtained when X_{22} is a positive value. Thus, in this chapter, the design factors are determined by (10-a) where X_{22} is a positive value.

Fig. 9 shows the input power factor according to R_L and m when X_{in}^* is designed to be zero at the rated condition. As shown in the figure, the load range where the power factor is maintained close to 1 becomes wider as the value of m is further from 1.

From (12), the input voltage-to-output voltage gain (G_v) and input voltage-to-output current gain (G_i) is expressed as

$$G_v = \frac{V_{o,dc}}{V_{in,dc}} = pf\sqrt{\frac{R_L^*}{R_{in}^*}}, \tag{13}$$

$$G_i = \frac{I_{o,dc}}{V_{in,dc}} = pf\sqrt{\frac{1}{R_L^* R_{in}^*}}. \tag{14}$$

From (13), the converter can keep the constant output voltage when the ratio between R_{in} and R_L is a constant value. This feature is achieved in $A1$ area where the value of m is much lower than 1. For this reason, the first design example P1 is designed in the area $A1$. On the other hand,

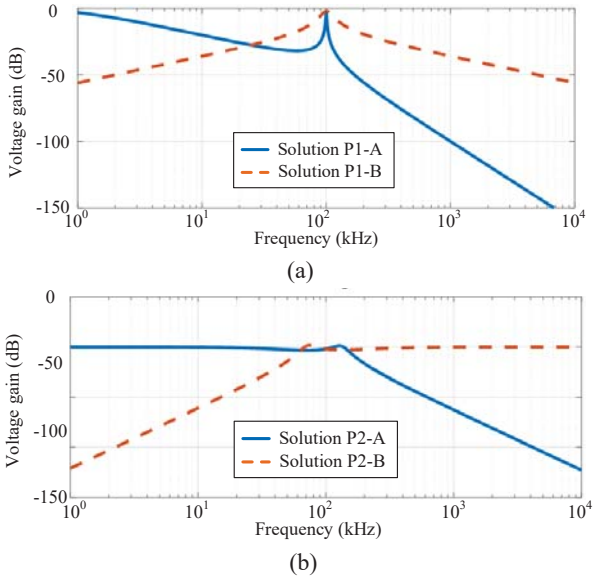

Fig. 10. Voltage gain curves for solution A and B of (a) P1 and (b) P2.

TABLE II
DESIGNED PARAMETERS

Prototype 1 (P1) / m=0.05	
Solution P1-A	*Solution P1-B*
X_1= 547.4 [Ω] (L_1= 871.3 [uH]) X_2= 438.0 [Ω] (L_2= 697.1 [uH]) X_3= -243.5[Ω] (C_3= 6.537 [nF])	X_1= 60.49 [Ω] (L_1= 96.27 [uH]) X_2= -48.94 [Ω] (C_2= 32.52 [nF]) X_3= 243.5 [Ω] (L_3= 387.5 [uH])
Prototype 2 (P2) / m=20	
Solution P2-A	*Solution P2-B*
X_1= 12.93 [Ω] (L_1= 20.59 [uH]) X_2= 12.66 [Ω] (L_2= 20.15 [uH]) X_3= -12.17 [Ω] (C_3= 130.7 [nF])	X_1= -11.41 [Ω] (C_1= 139.4 [nF]) X_2= -11.69 [Ω] (C_2= 136.2 [nF]) X_3= 12.17 [Ω] (L_3= 19.38 [uH])

the product of R_{in} and R_L is almost constant in the area $A3$ where the value of m is much higher than 1. (14) shows that this characteristic allows the converter to maintain the constant output current. Therefore, the second design example P2 is designed in the area $A3$.

In this paper, the value of m is set to 0.05 for P1 and 20 for P2 respectively. Consequently, the values of X_1, X_2, and X_3 are determined by (10-a) and (11) as shown in Table II. It is noticeable that there are two possible solutions (Solution A and Solution B) to choose X_3 for each design example. Since the fundamental harmonic approximation (FHA) is used in the analysis, it is necessary to make sure whether these solutions actually satisfy the assumption or not. Fig. 10(a) and (b) show the voltage gain curve of P1 and P2 respectively. As shown in Fig. 10(a), both solutions ensure the sufficient harmonic attenuation. Thus, in both solutions, the converter is designed as intended. On the other hand, as shown in Fig. 10(b), solution B is not applicable for realization since the harmonic components are not sufficiently attenuated. Therefore, solution A is selected to implement the design example of P2.

B. Simulation results

Fig. 11 and Fig. 12 shows the simulation results of the design example P1. Fig. 11(a) and (b) show the dc-output voltage ($V_{o,dc}$) and dc-output current ($I_{o,dc}$) according to the load condition. The load condition is changed from 100% to

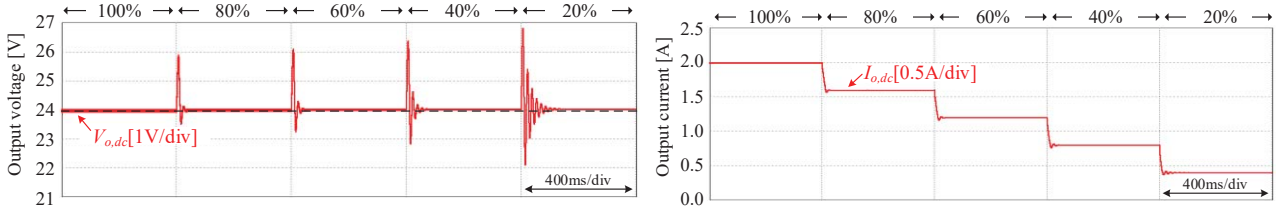

(a) (b)

Fig. 11. (a)The output voltage ($V_{o,dc}$) and (b)the output current ($I_{o,dc}$) of P1 according to the load condition.

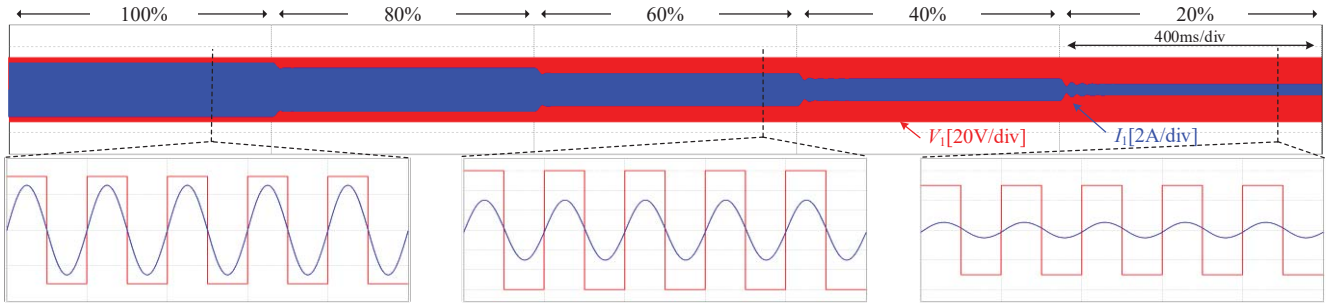

Fig. 12. The waveforms of the input current (I_1) and the input voltage (V_1) of P1 according load condition.

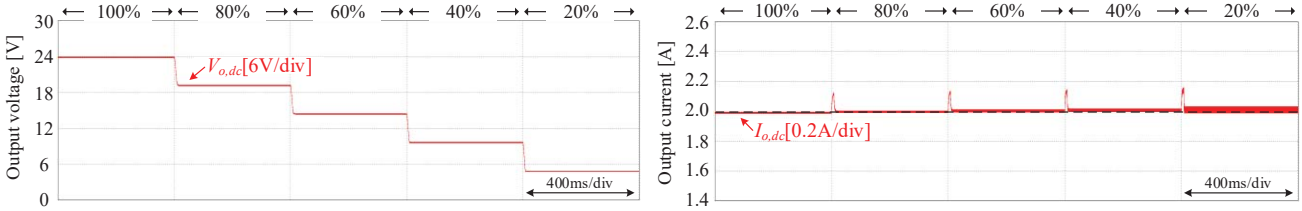

(a) (b)

Fig. 13. (a)The output voltage ($V_{o,dc}$) and (b)the output current ($I_{o,dc}$) of P2 according to the load condition.

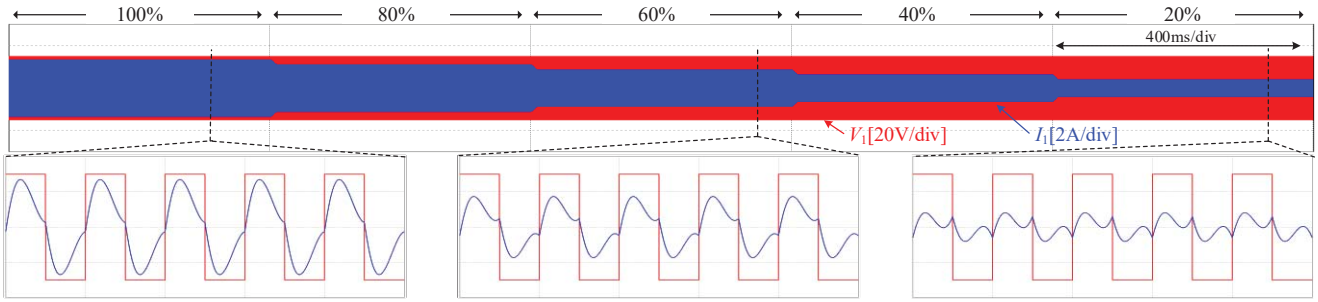

Fig. 14. The waveforms of the input current (I_1) and the input voltage (V_1) of P1 according load condition.

20% sequentially. As expected, when the output power changes, $V_{o,dc}$ remain at a substantially constant value within the given load range, and instead $I_{o,dc}$ varies with the output power. Fig.12 shows the waveforms of the input current (I_1) and the input voltage (V_1) according to load condition. Since the converter is designed in $A1$, the input reactance remain close to zero. In fact, the input reactance slightly increases to a positive value as the load decreases due to the impedance characteristics of area $A1$. Thus, the converter satisfies the ZVS condition while the power factor is maintained to nearly unity (0.9~1.0) for the given load range.

Fig. 13 and Fig. 14 shows the simulation results of the design example P2. Fig. 13(a) and (b) show the dc-output voltage ($V_{o,dc}$) and dc-output current ($I_{o,dc}$) according to load condition. In this case, $I_{o,dc}$ remains a nearly constant value within the given load range when the load changes from 100% to 20%. Fig.14 shows the waveforms of the input current (I_1) and the input voltage (V_1) according to load condition. Here, the harmonic components are included in the input current, but the converter still satisfies the ZVS condition. Since the converter is designed in $A3$, it can be seen that there is little variation in the input reactance of the fundamental component for the given load range.

IV. Conclusion

This paper presents the method for designing and evaluating resonant networks at a single frequency through a two-port network analysis. This paper shows that arbitrary load impedance can be converted to desired input impedance through a two-port network composed of passive elements. Through this analysis, the resonant network of the converter is designed under the rated condition. Furthermore, it is revealed that there is one degree of freedom that can optimize the network, and it is used to investigate some noticeable characteristics against load variation. In order to verify the proposed concept, two design examples are introduced and simulation results are presented.

ACKNOWLEDGMENT

This work was supported by the Seoul National University Electric Power Research Institute (SEPRI).

This work was supported by the Global Frontier R&D Program on Center for Multiscale Energy System funded by the National Research Foundation under the Ministry of Science, ICT & Future Planning, Korea. (2012M3A6A7054855).

REFERENCES

[1] R. P. Severns, "Topologies for three-element resonant converters," in *IEEE Trans. on Power Electron.*, vol. 7, no. 1, pp. 89-98, Jan 1992.

[2] I. Batarseh, "Resonant converter topologies with three and four energy storage elements," in *IEEE Trans. on Power Electron.*, vol. 9, no. 1, pp. 64-73, Jan 1994.

[3] A. Khoshsaadat and J. S. Moghani, "Fifth-Order T-Type Passive Resonant Tanks Tailored for Constant Current Resonant Converters," in *IEEE Trans.* on *Circuits Syst. I: Reg. Papers*, vol. 65, no. 2, pp. 842-853, Feb. 2018.

[4] D. Huang, F. C. Lee and D. Fu, "Classification and selection methodology for multi-element resonant converters," in *Proc. IEEE APEC*, 2011, pp. 558-565.

[5] M. T. Outeiro, G. Buja and D. Czarkowski, "Resonant Power Converters: An Overview with Multiple Elements in the Resonant Tank Network," in *IEEE Ind. Electron. Mag.*, vol. 10, no. 2, pp. 21-45, June 2016.

[6] M. Borage, K. V. Nagesh, M. S. Bhatia and S. Tiwari, "Resonant Immittance Converter Topologies," in *IEEE Trans. on Ind. Electron.*, vol. 58, no. 3, pp. 971-978, March 2011.

[7] X. Tan and X. Ruan, "Equivalence Relations of Resonant Tanks: A New Perspective for Selection and Design of Resonant Converters," in *IEEE Trans. on Ind. Electron.*, vol. 63, no. 4, pp. 2111-2123, April 2016.

[8] Y. Han, O. Leitermann, D. A. Jackson, J. M. Rivas and D. J. Perreault, "Resistance Compression Networks for Radio-Frequency Power Conversion," in *IEEE Trans. on Power Electron.*, vol. 22, no. 1, pp. 41-53, Jan. 2007.

[9] M. Danilovic, K. D. T. Ngo, and Z. Zhang, "Compression of the load resistance range in constant frequency resonant inverters," in *Proc. IEEE ECCE*, 2014, pp. 2793-2800.